

Confronting the Ellipsoidal Universe to the Planck 2018 Data ¹

Paolo Cea ²

INFN - Sezione di Bari, Via Amendola 173 - 70126 Bari, Italy

Abstract

We compared the Planck 2018 data on the large-scale anisotropies in the cosmic microwave background to the results obtained in the slightly anisotropic ellipsoidal universe. We focused on the quadrupole temperature correlations to better constrain the eccentricity at decoupling and the direction of the symmetry axis. We found that the quadrupole TE and EE temperature correlations in the ellipsoidal universe are still in reasonable agreement with the Planck 2018 data. We suggested that an experimental estimate of the average large-scale polarisation by the Planck Collaboration could confirm or reject the anisotropic universe proposal.

keywords: cosmic microwave radiation; cosmology: theory

PACS: 98.70.Vc; 98.80.-k

¹Based on observations obtained with Planck (<http://www.esa.int/Planck>), an ESA science mission with instruments and contributions directly funded by ESA Member States, NASA, and Canada.

²Electronic address: paulo.cea@ba.infn.it

1 Introduction

The temperature anisotropies in the cosmic microwave background (CMB) is one of the most powerful way to study cosmology and the physics of the early Universe. Recently, the Planck Collaboration reported the final results on the CMB anisotropies [1, 2, 3, 4, 5, 6, 7, 8, 9] confirming the cosmological Lambda Cold Dark Matter (Λ CDM) model to the highest level of accuracy. Nevertheless, even the Planck 2018 data are confirming the presence of anomalous features at large scales. The most evident anomaly concerns the quadrupole temperature correlation that is still heavily suppressed with respect to the best-fit standard cosmological Λ CDM model. There are several proposals in the literature to cope with the suppression of power at large scales in the CMB anisotropies. In particular, it has been suggested [10, 11] that, if one admits that the large-scale spatial geometry of our universe could be only plane-symmetric, then the quadrupole amplitude can be drastically reduced without affecting higher multipoles of the angular power spectrum of the temperature anisotropies. If this is the case, then the metric of the Friedmann-Robertson-Walker (FRW) standard cosmological model (see, for instance, Ref. [12]) ³:

$$ds^2 = -dt^2 + a^2(t)\delta_{ij} dx^i dx^j , \quad (1.1)$$

should be replaced with the ellipsoidal universe metric:

$$ds^2 = -dt^2 + a^2(t)(\delta_{ij} + h_{ij}) dx^i dx^j , \quad (1.2)$$

where h_{ij} is a metric perturbation:

$$h_{ij} = -e^2(t) n_i n_j , \quad (1.3)$$

where $e(t)$ is the ellipticity and the unit vector \vec{n} determines the direction of the symmetry axis. In fact, the ellipsoidal universe corresponds to a Bianchi type I [13] cosmological model with planar symmetry. It is known since long time [14, 15, 16, 17] that anisotropic cosmological models in general induce at large scales sizeable E- and B-mode polarisation in the the cosmic microwave background radiation. Actually, the recent results [18] of a joint analysis of CMB data from BICEP2/Keck Array and Planck Collaborations found no statistically significant evidence of primordial B-modes. This should select Bianchi type I cosmological models as viable anisotropic cosmological models since B-mode polarisation is being produced in all Bianchi types except type I. Indeed, in our previous papers [19, 20] we showed that the ellipsoidal geometry of the universe could induce sizeable linear polarisation signal at large scales without invoking reionization processes. In particular, in Ref. [20] we evaluated the quadrupole TE and EE correlations and compared with the WMAP nine-year data [21, 22]. The aim of the present paper is to critically contrast the CMB quadrupole correlations evaluated in the ellipsoidal universe with the recent Planck 2018 data.

The plan of the paper is as follows. In sect. 2 we summarise the main results presented in Ref. [20]; sect. 3 is devoted to the calculations of the quadrupole correlations and, by using the Planck 2018 data, to better constrain the eccentricity at decoupling and the symmetry axis. We also compare in sect. 3.1 the quadrupole TE and EE correlations to the Planck data. Finally, in sect. 4 we summarise the main results of the present paper and we draw our conclusions.

³We shall use throughout the natural units $c = 1$, $\hbar = 1$, $k_B = 1$.

2 The CMB large scale anisotropies

In this section, for later convenience, we summarise the calculations of the large scale temperature anisotropies in the ellipsoidal universe [10, 11] presented in Ref. [20].

Let us consider the Boltzmann equation for the photon distribution in the ellipsoidal universe by taking into account also the effects of the cosmological inflation produced primordial scalar perturbations. The temperature anisotropies caused by the inflation produced primordial scalar perturbations are discussed in textbooks (see, for instance, Refs. [23], [24]). Here, we consider the primordial scalar perturbations induced by the inflation. In the conformal Newtonian gauge [24] the effects of these perturbations on the metrics are accounted for by two functions $\Psi(\vec{x}, t)$ and $\Phi(\vec{x}, t)$ corresponding to the Newtonian potential and the perturbation to the spatial curvature, respectively. Therefore, in the ellipsoidal universe the perturbed metrics reads:

$$ds^2 = -[1 + 2\Psi(\vec{x}, t)] dt^2 + a^2(t) \{ \delta_{ij} [1 + 2\Phi(\vec{x}, t)] + h_{ij} \} dx^i dx^j . \quad (2.1)$$

We need to evaluate the temperature fluctuations of the cosmic background radiation induced by eccentricity of the universe and by the inflation produced primordial cosmological perturbations. We assume that the photon distribution function $f(\vec{x}, t)$ is an isotropically radiating blackbody at a sufficiently early epoch. The subsequent evolution of $f(\vec{x}, t)$ is determined by the Boltzmann equation [23, 24]:

$$\frac{df}{dt} = \left(\frac{\partial f}{\partial t} \right)_{coll} , \quad (2.2)$$

where $(\frac{\partial f}{\partial t})_{coll}$ is the collision integral which takes care of Thomson scatterings between matter and radiation. The distribution function depends on the space-time point x^μ and the momentum vector p^μ :

$$p^\mu = \frac{dx^\mu}{d\lambda} , \quad (2.3)$$

where λ parametrises the particle's path. Actually, we may consider the distribution function as a function of the magnitude of momentum p and the momentum direction \hat{p}^i , $\delta_{ij} \hat{p}^i \hat{p}^j = 1$. Tacking into account the metric Eq. (2.1) one gets [20]:

$$\frac{df}{dt} \simeq \frac{\partial f}{\partial t} + \frac{\hat{p}^i}{a(t)} \frac{\partial f}{\partial x^i} - p \frac{\partial f}{\partial p} [H(t) + \frac{\partial \Phi}{\partial t} + \frac{\hat{p}^i}{a(t)} \frac{\partial \Psi}{\partial x^i} + \frac{1}{2} \hat{p}^i \hat{p}^j \frac{\partial h_{ij}}{\partial t}] , \quad (2.4)$$

where $H = \dot{a}/a$ is the Hubble rate. Now, the photon distribution perturbed with respect to its zero-order Bose-Einstein value:

$$f_0(p, t) = \frac{1}{e^{\frac{p}{T(t)}} - 1} , \quad (2.5)$$

can be written as:

$$f(\vec{x}, t, p, \hat{p}) = \frac{1}{e^{\frac{p}{T(t)[1 + \Theta(\vec{x}, t, p, \hat{p})]}} - 1} . \quad (2.6)$$

After expanding to the first order in the perturbation $\Theta(\vec{x}, t, p, \hat{p})$ we get:

$$f(\vec{x}, t, p, \hat{p}) \simeq f_0(p, t) [1 + \Theta(\vec{x}, t, p, \hat{p})] . \quad (2.7)$$

Note that from Eq. (2.6) it follows that the distribution function $\Theta(\vec{x}, t, p, \hat{p})$ is the temperature contrast function:

$$\Theta(\vec{x}, t, p, \hat{p}) = \frac{\Delta T(\vec{x}, t, p, \hat{p})}{T(t)}. \quad (2.8)$$

The perturbed distribution $\Theta(\vec{x}, t, p, \hat{p})$ can be obtained by solving the Boltzmann equation to the first order. In this approximation we obtain:

$$\frac{\partial \Theta}{\partial t} + \frac{\hat{p}^i}{a(t)} \frac{\partial \Theta}{\partial x^i} + \frac{\partial \Phi}{\partial t} + \frac{\hat{p}^i}{a(t)} \frac{\partial \Psi}{\partial x^i} + \frac{1}{2} \hat{p}^i \hat{p}^j \frac{\partial h_{ij}}{\partial t} \simeq \frac{1}{f_0} \left(\frac{\partial f}{\partial t} \right)_{coll}. \quad (2.9)$$

In the same approximations the collision integral is a linear functional of $\Theta(\vec{x}, t, p, \hat{p})$. Moreover, we showed [20] that at large scales the collision integral can be considered a linear homogeneous functional of the distribution function $\Theta(\vec{x}, t, p, \hat{p})$. Therefore, writing:

$$\Theta(\vec{x}, t, p, \hat{p}) \simeq \Theta^A(\vec{x}, t, p, \hat{p}) + \Theta^I(\vec{x}, t, p, \hat{p}), \quad (2.10)$$

we have:

$$\left(\frac{\partial f}{\partial t} \right)_{coll} [\Theta] \simeq \left(\frac{\partial f}{\partial t} \right)_{coll} [\Theta^A] + \left(\frac{\partial f}{\partial t} \right)_{coll} [\Theta^I]. \quad (2.11)$$

In fact, Eqs. (2.10) and (2.11) show that Θ^A and Θ^I are the temperature fluctuations induced by the spatial anisotropy of the geometry of the universe and by the scalar perturbations generated during the inflation, respectively. Accordingly we obtain:

$$\frac{\partial \Theta^I}{\partial t} + \frac{\hat{p}^i}{a(t)} \frac{\partial \Theta^I}{\partial x^i} + \frac{\partial \Phi}{\partial t} + \frac{\hat{p}^i}{a(t)} \frac{\partial \Psi}{\partial x^i} \simeq \frac{1}{f_0} \left(\frac{\partial f}{\partial t} \right)_{coll} [\Theta^I], \quad (2.12)$$

and

$$\frac{\partial \Theta^A}{\partial t} + \frac{\hat{p}^i}{a(t)} \frac{\partial \Theta^A}{\partial x^i} + \frac{1}{2} \hat{p}^i \hat{p}^j \frac{\partial h_{ij}}{\partial t} \simeq \frac{1}{f_0} \left(\frac{\partial f}{\partial t} \right)_{coll} [\Theta^A]. \quad (2.13)$$

It is worthwhile to stress that our results imply that at large scales:

$$\Delta T(\vec{x}, t, p, \hat{p}) \simeq \Delta T^A(\vec{x}, t, p, \hat{p}) + \Delta T^I(\vec{x}, t, p, \hat{p}), \quad (2.14)$$

where ΔT^I and ΔT^A are the temperature fluctuations induced by the cosmological scalar perturbations and by the spatial anisotropy of the metric of the universe.

To determine the CMB temperature fluctuations at large scales we need to solve the Boltzmann equations Eqs. (2.12) and (2.13). Eq. (2.12) is the Boltzmann equation of the standard Λ CDM cosmological model, and it has been extensively discussed in literature. As a consequence, we only need to solve the Boltzmann equation Eq. (2.13) which allows us to find the CMB temperature fluctuations caused by the anisotropy of the geometry of the universe. To this end, we introduce the Fourier transform of the temperature contrast function:

$$\Theta^A(\vec{x}, t, p, \hat{p}) = \int \frac{d^3 k}{(2\pi)^3} e^{i \vec{k} \cdot \vec{x}} \Theta^A(\vec{k}, t, p, \hat{p}). \quad (2.15)$$

Considering that the collision integral depends linearly on Θ^A , we have:

$$\frac{\partial \Theta^A(\vec{k}, t, p, \hat{p})}{\partial t} + \frac{i \vec{k} \cdot \hat{p}}{a(t)} \Theta^A(\vec{k}, t, p, \hat{p}) + \frac{1}{2} \hat{p}^i \hat{p}^j \frac{\partial h_{ij}}{\partial t} \simeq \frac{1}{f_0} \left(\frac{\partial f}{\partial t} \right)_{coll} [\Theta^A(\vec{k}, t, p, \hat{p})]. \quad (2.16)$$

To determine the polarisation of the cosmic microwave background we need the polarised distribution function which, in general, is represented by a column vector whose components are the four Stokes parameters [25]. In fact, due to the axial symmetry of the metric only two Stokes parameters need to be considered, namely the two intensities of radiation with electric vectors in the plane containing \vec{p} and \vec{n} and perpendicular to this plane respectively. As a consequence, Eq. (2.7) is replaced by:

$$f(\vec{x}, t, p, \hat{p}) \simeq f_0(p, t) \left[\begin{pmatrix} 1 \\ 1 \end{pmatrix} + \Theta^A(\vec{x}, t, p, \hat{p}) \right], \quad (2.17)$$

where, now, $\Theta^A(\vec{x}, t, p, \hat{p})$ should be regarded as a two component column vector. Defining

$$\mu = \cos \theta_{\vec{p}\vec{n}}, \quad \cos \theta_{\vec{k}\vec{p}} = \frac{\vec{k} \cdot \hat{p}}{k}, \quad (2.18)$$

we get from Eq. (2.16):

$$\begin{aligned} \frac{\partial \Theta^A(\vec{k}, t, \mu)}{\partial t} + \frac{i k}{a(t)} \cos \theta_{\vec{k}\vec{p}} \Theta^A(\vec{k}, t, \mu) &\simeq \frac{1}{2} \left[\frac{d}{dt} e^2(t) \right] \mu^2 \begin{pmatrix} 1 \\ 1 \end{pmatrix} \\ - \sigma_T n_e \left[\Theta^A(\vec{k}, t, \mu) - \frac{3}{8} \int_{-1}^1 \begin{pmatrix} 2(1 - \mu^2)(1 - \mu'^2) + \mu^2 \mu'^2 & \mu^2 \\ \mu'^2 & 1 \end{pmatrix} \Theta^A(\vec{k}, t, \mu') d\mu' \right] \end{aligned} \quad (2.19)$$

where σ_T is the Thomson cross section and $n_e(t)$ the electron number density [25]. After introducing the conformal time:

$$\eta(t) = \int_0^t \frac{dt'}{a(t')}, \quad (2.20)$$

Eq. (2.19) can be written as:

$$\begin{aligned} \frac{\partial \Theta^A(\vec{k}, \eta, \mu)}{\partial \eta} + i k \cos \theta_{\vec{k}\vec{p}} \Theta^A(\vec{k}, \eta, \mu) &\simeq \frac{1}{2} \left[\frac{d}{d\eta} e^2(\eta) \right] (\mu^2 - \frac{1}{3}) \begin{pmatrix} 1 \\ 1 \end{pmatrix} \\ - a(\eta) \sigma_T n_e \left[\Theta^A(\vec{k}, \eta, \mu) - \frac{3}{8} \int_{-1}^1 \begin{pmatrix} 2(1 - \mu^2)(1 - \mu'^2) + \mu^2 \mu'^2 & \mu^2 \\ \mu'^2 & 1 \end{pmatrix} \Theta^A(\vec{k}, \eta, \mu') d\mu' \right]. \end{aligned} \quad (2.21)$$

The solutions of Eq. (2.21) are given by [16, 19, 20]:

$$\Theta^A(\vec{k}, \eta, \mu) = \theta_a(\vec{k}, \eta) (\mu^2 - \frac{1}{3}) \begin{pmatrix} 1 \\ 1 \end{pmatrix} + \theta_p(\vec{k}, \eta) (1 - \mu^2) \begin{pmatrix} 1 \\ -1 \end{pmatrix}. \quad (2.22)$$

It turns out that $\theta_a(\vec{k}, \eta)$ measures the degree of anisotropy, while $\theta_p(\vec{k}, \eta)$ gives the polarisation of the primordial radiation. In Ref. [20] we found:

$$\theta_a(\vec{k}, \eta) = \frac{1}{7} \int_{\eta_i}^{\eta} \Delta H(\eta') \left[6e^{-\tau(\eta, \eta')} + e^{-\frac{3}{10}\tau(\eta, \eta')} \right] e^{i k \cos \theta_{\vec{k}\vec{p}}(\eta' - \eta)} d\eta', \quad (2.23)$$

$$\theta_p(\vec{k}, \eta) = \frac{1}{7} \int_{\eta_i}^{\eta} \Delta H(\eta') \left[e^{-\tau(\eta, \eta')} - e^{-\frac{3}{10}\tau(\eta, \eta')} \right] e^{i k \cos \theta_{\vec{k}\vec{p}}(\eta' - \eta)} d\eta', \quad (2.24)$$

where we introduced the cosmic shear [15, 19, 20]:

$$\Delta H(\eta) \equiv \frac{1}{2} \frac{d}{d\eta} e^2(\eta) , \quad (2.25)$$

and the optical depth:

$$\tau(\eta, \eta') = \int_{\eta'}^{\eta} \sigma_T n_e a(\eta'') d\eta'' . \quad (2.26)$$

To a good approximation, we showed that [20]:

$$\Theta(\vec{k}, \eta_0, \mu, \hat{p}) \simeq \theta_a \left(\mu^2 - \frac{1}{3} \right) e^{-i k \cos \theta_{\vec{k}\hat{p}} \eta_0} \begin{pmatrix} 1 \\ 1 \end{pmatrix} + \theta_p (1 - \mu^2) e^{-i k \cos \theta_{\vec{k}\hat{p}} \eta_0} \begin{pmatrix} 1 \\ -1 \end{pmatrix} , \quad (2.27)$$

where η_0 is the conformal time at the present time. Moreover, we also found:

$$\theta_p \simeq 8.92 \cdot 10^{-3} e_{\text{dec}}^2 . \quad (2.28)$$

and

$$\theta_a = -\frac{1}{2} \epsilon , \quad \epsilon \simeq 0.944 e_{\text{dec}}^2 . \quad (2.29)$$

where e_{dec} is the ellipticity at decoupling.

3 The quadrupole correlations

The temperature anisotropies of the cosmic background depend on the polar angle θ, ϕ , so that one usually expands in terms of spherical harmonics:

$$\Delta T(\theta, \phi) = \sum_{\ell=1}^{\infty} \sum_{m=-\ell}^{+\ell} a_{\ell m} Y_{\ell m}(\theta, \phi) . \quad (3.1)$$

The CMB temperature fluctuations can be fully characterised by the power spectrum:

$$(\Delta T_{\ell})^2 \equiv \mathcal{D}_{\ell} = \frac{\ell(\ell+1)}{2\pi} C_{\ell} , \quad C_{\ell} = \frac{1}{2\ell+1} \sum_{m=-\ell}^{+\ell} |a_{\ell m}|^2 . \quad (3.2)$$

In particular, the quadrupole anisotropy refers to the multipole $\ell = 2$. Remarkably, also the Planck 2018 data [26] confirmed that the observed quadrupole anisotropy:

$$(\Delta T_2)^2 = \mathcal{D}_2 \simeq 225.9 \mu K^2 , \quad (3.3)$$

is much smaller than the quadrupole anisotropy expected according to the ' TT, TE, EE + low E + lensing ' best fit Λ CDM model to the Planck 2018 data [26]:

$$(\Delta T_2^I)^2 = 1017 \pm 643 \mu K^2 . \quad (3.4)$$

Note that in Eq. (3.4) the uncertainty is due to the so-called cosmic variance [23] that, in fact, should be included in the theoretical expectations.

In the standard cosmological model the CMB temperature fluctuations are induced by the cosmological perturbations of the FRW homogeneous and isotropic background metric

generated by the inflation-produced potentials. In the ellipsoidal universe we must also consider the effects on the CMB anisotropies induced by the anisotropic expansion of the universe. It turned out [19, 20] that, as discussed in sec. 2, at large scales the observed anisotropies in the CMB temperature are due to the linear superposition of the two contributions according to Eq. (2.14). Following Ref. [20], let us introduce the dimensionless temperature anisotropies:

$$\frac{\Delta T(\theta, \phi)}{T_0} = \sum_{\ell=1}^{\infty} \sum_{m=-\ell}^{+\ell} a_{\ell m} Y_{\ell m}(\theta, \phi) , \quad (3.5)$$

where $T_0 \simeq 2.7255 \text{ K}$ [27] is the actual (average) temperature of the CMB radiation. Obviously, the $a_{\ell m}$'s in Eq. (3.5) are dimensionless and can be obtained from the corresponding coefficients in Eq. (3.1) by dividing by T_0 . After that, one introduces the power spectrum:

$$\left(\frac{\Delta T_{\ell}}{T_0}\right)^2 = \frac{1}{2\pi} \frac{\ell(\ell+1)}{2\ell+1} \sum_m |a_{\ell m}|^2 , \quad (3.6)$$

that fully characterises the properties of the CMB temperature anisotropy. We have seen that at large scales the temperature fluctuations ΔT are the sum of the temperature fluctuations ΔT^I induced by the cosmological inflation perturbations and the temperature fluctuations ΔT^A due to the spatial anisotropy of the metric of the universe. Writing:

$$\frac{\Delta T^I(\theta, \phi)}{T_0} = \sum_{\ell=1}^{\infty} \sum_{m=-\ell}^{+\ell} a_{\ell m}^I Y_{\ell m}(\theta, \phi) , \quad (3.7)$$

and

$$\frac{\Delta T^A(\theta, \phi)}{T_0} = \sum_{\ell=1}^{\infty} \sum_{m=-\ell}^{+\ell} a_{\ell m}^A Y_{\ell m}(\theta, \phi) , \quad (3.8)$$

we have:

$$a_{\ell m} = a_{\ell m}^A + a_{\ell m}^I . \quad (3.9)$$

In our previous paper [20] we argued that the main contributions of the anisotropy of the metric to the CMB temperature anisotropies are for $\ell = 2$. Therefore we are led to consider the quadrupole anisotropy $\ell = 2$. Firstly, let us consider the contributions to temperature contrast function induced by the anisotropic expansion of the universe. Since at large scales we may neglect the spatial dependence of the contrast function, we may set $k \simeq 0$ in Eq. (2.27). In this case we obtain at once:

$$\frac{\Delta T^A(\theta, \phi)}{T_0} \simeq \Theta^A(\vec{k} \simeq 0, \eta_0, \mu, \hat{p}) = \theta_a \left(\cos^2 \theta_{\vec{p}\vec{n}} - \frac{1}{3} \right) , \quad (3.10)$$

where θ_a is given by Eq. (2.28) and θ, ϕ are the polar angles of the photon momentum \vec{p} . Let θ_n, ϕ_n be the polar angles of the direction of the axis of symmetry \vec{n} , then:

$$\frac{\Delta T^A(\theta, \phi)}{T_0} \simeq \frac{2}{3} \theta_a P_2(\cos \theta_{\vec{p}\vec{n}}) = \frac{2}{3} \theta_a \frac{4\pi}{5} \sum_{m=-2}^{+2} Y_{2m}(\theta, \phi) Y_{2m}^*(\theta_n, \phi_n) . \quad (3.11)$$

As a consequence, we get:

$$a_{2m}^A \simeq -\frac{4\pi}{15} \epsilon^2 Y_{\ell m}^*(\theta_n, \phi_n) \ , \ a_{\ell m}^A = 0 \text{ for } \ell \neq 2 \ . \quad (3.12)$$

From Eq. (3.12) one easily finds:

$$\begin{aligned} a_{20}^A &\simeq +\frac{1}{6} \epsilon^2 \sqrt{\frac{\pi}{5}} [1 + 3 \cos^2(2\theta_n)] \ , \\ a_{21}^A &= (a_{2,-1}^A)^* \simeq +i \sqrt{\frac{\pi}{30}} \epsilon^2 e^{-i\phi_n} \sin(2\theta_n) \ , \\ a_{22}^A &= (a_{2,-2}^A)^* \simeq +\sqrt{\frac{\pi}{30}} \epsilon^2 e^{-2i\phi_n} \sin^2 \theta_n \ . \end{aligned} \quad (3.13)$$

After defining the quadrupole anisotropy:

$$\mathcal{Q}_A^2 \equiv \left(\frac{\Delta T_2^A}{T_0} \right)^2 \ , \quad (3.14)$$

one finds:

$$\mathcal{Q}_A \simeq \frac{2}{5\sqrt{3}} \epsilon^2 \ . \quad (3.15)$$

Concerning the observed quadrupole temperature anisotropy, we introduce:

$$\mathcal{Q}^2 \equiv \left(\frac{\Delta T_2}{T_0} \right)^2 \ , \quad (3.16)$$

so that, according to Eq. (3.9), we have:

$$\mathcal{Q}^2 = \frac{3}{5\pi} \sum_{m=-2}^{m=+2} |a_{2m}^A + a_{2m}^I|^2 \ . \quad (3.17)$$

We see that to determine \mathcal{Q}^2 we need the $a_{\ell m}^I$'s. Since the standard inflation-produced temperature fluctuations are statistically isotropic, we can write [11, 20]:

$$\begin{aligned} a_{20}^I &\simeq \sqrt{\frac{\pi}{3}} \mathcal{Q}_I \ , \\ a_{21}^I &= -(a_{2,-1}^I)^* \simeq +i \sqrt{\frac{\pi}{3}} e^{i\phi_1} \mathcal{Q}_I \ , \\ a_{22}^I &= (a_{2,-2}^I)^* \simeq \sqrt{\frac{\pi}{3}} e^{i\phi_2} \mathcal{Q}_I \ , \end{aligned} \quad (3.18)$$

where $0 \leq \phi_1, \phi_2 \leq 2\pi$ are unknown phases and \mathcal{Q}_I , defined by

$$\mathcal{Q}_I^2 \equiv \left(\frac{\Delta T_2^I}{T_0} \right)^2 \ , \quad (3.19)$$

can be easily estimated from Eq. (3.4):

$$\mathcal{Q}_I \simeq (11.70 \pm 3.70) 10^{-6} \ . \quad (3.20)$$

As a consequence we get for the total quadrupole anisotropy:

$$\mathcal{Q}^2 = \mathcal{Q}_A^2 + \mathcal{Q}_I^2 + 2 f(\theta_n, \phi_n, \phi_1, \phi_2) \mathcal{Q}_A \mathcal{Q}_I , \quad (3.21)$$

where [10, 11, 20]:

$$f(\theta_n, \phi_n, \phi_1, \phi_2) = \frac{1}{4\sqrt{5}} [1 + 3 \cos(2\theta_n)] + \sqrt{\frac{3}{10}} \sin(2\theta_n) \cos(\phi_1 + \phi_n) + \sqrt{\frac{3}{10}} \sin^2 \theta_n \cos(\phi_2 + 2\phi_n) . \quad (3.22)$$

Equations (3.21) and (3.22) suggest that, if the space-time background metric is not isotropic, the quadrupole anisotropy may become smaller than the one expected in the standard isotropic Λ CDM cosmological model. To see this, we note that:

$$a_{20} \simeq + \sqrt{\frac{\pi}{3}} \mathcal{Q}_I + \frac{1}{6} \epsilon^2 \sqrt{\frac{\pi}{5}} [1 + 3 \cos^2(2\theta_n)] , \quad (3.23)$$

$$a_{21} = +i \sqrt{\frac{\pi}{3}} e^{i\phi_1} \mathcal{Q}_I + i \sqrt{\frac{\pi}{30}} \epsilon^2 e^{-i\phi_n} \sin(2\theta_n) , \quad (3.24)$$

$$a_{22} \simeq + \sqrt{\frac{\pi}{3}} e^{i\phi_2} \mathcal{Q}_I + \sqrt{\frac{\pi}{30}} \epsilon^2 e^{-2i\phi_n} \sin^2 \theta_n . \quad (3.25)$$

Indeed, the quadrupole anomalies can be accounted for if:

$$a_{21} \approx 0 \quad , \quad |a_{20}|^2 \ll 2 |a_{22}|^2 . \quad (3.26)$$

It turned out that Eq. (3.26) allowed us to determine the eccentricity at decoupling and constraint the polar angles of the symmetry axis [20]:

$$\epsilon^2 \simeq \frac{\sqrt{10} \mathcal{Q}_I}{|\sin(2\theta_n)|} , \quad (3.27)$$

and

$$\theta_n \simeq \arctan \left(\pm \frac{\sqrt{6}}{2} + 2 \right) . \quad (3.28)$$

Using Eqs. (3.21), (3.27) and Eq. (3.28) we reach an estimate of the eccentricity at decoupling a little bit smaller than in Ref. [20]:

$$e_{\text{dec}} \simeq (8.32 \pm 1.32) 10^{-3} . \quad (3.29)$$

As concern the quadrupole temperature anisotropy, we have:

$$\mathcal{Q}^2 \simeq \frac{6}{5\pi} |a_{22}|^2 \simeq \frac{2}{5} \mathcal{Q}_I^2 \left[1 + \frac{\sin^4 \theta_n}{\sin^2(2\theta_n)} + \frac{2 \sin^2 \theta_n}{|\sin(2\theta_n)|} \cos(\phi_2 + 2\phi_n) \right] . \quad (3.30)$$

The observed value of the quadrupole temperature anisotropy is recovered if:

$$\cos(\phi_2 + 2\phi_n) \simeq -0.944_{-0.056}^{+0.109} . \quad (3.31)$$

To summarise, we have shown that the anomalous low quadrupole temperature anisotropy can be reconciled with observations in the ellipsoidal universe by allowing a rather small

eccentricity at decoupling. On the other hand, in our previous paper [20], we found that the anisotropy of the metric contributes mainly at large scales affecting only the low-lying multipoles, at least for the temperature-temperature anisotropy correlations. So that the ellipsoidal cosmological model can reproduce the observed quadrupole temperature correlation without spoiling the excellent agreement of the standard cosmological model with the TT correlations for $\ell > 2$. Finally, note that for the galactic coordinates b_n, l_n of the symmetry axis we have $b_n \simeq \pm 17^\circ$ while the longitude l_n is poorly constrained. It is worthwhile to observe that the full mission Planck temperature data exhibit an anomalous mirror antisymmetry in the direction $(b, l) \simeq (-17^\circ, 264^\circ)$ [28]. Remarkably, the galactic coordinates of the mirror antisymmetry direction are consistent with the allowed range of b_n, l_n . This lead us to identify that direction with the direction of the axis of symmetry. Therefore, we may safely assume:

$$\theta_n \simeq \arctan \left(2 - \frac{\sqrt{6}}{2} \right) \simeq 73^\circ \quad , \quad \phi_n \simeq 264^\circ . \quad (3.32)$$

Now we turn on the large scale polarisation in the primordial cosmic background. In our previous work [19] we argued that the ellipsoidal geometry of the universe induces sizeable polarisation signal at large scale without needing the CMB reionization mechanism. We will assume, therefore, that early CMB reionization is negligible. As a consequence, as it is well known [23, 24], at large scales the primordial inflation induced cosmological perturbations do not produce sizeable polarisation signal. In this case the polarisation of the temperature fluctuations are fully accounted for by the anisotropic expansion of the universe. According to our previous discussion, we have:

$$\Theta^E(\vec{k}, \eta_0, \mu, \hat{p}) \simeq \theta_p (1 - \cos^2 \theta_{\vec{p}\vec{n}}) e^{-i k \cos \theta_{\vec{k}\vec{p}} \eta_0} , \quad (3.33)$$

where the superscript E indicates that the temperature polarisation contributes only to the so-called E-modes. At large scales the main contributions to the polarisation temperature contrast functions are for $k \simeq 0$:

$$\frac{\Delta T^E(\theta, \phi)}{T_0} \simeq \Theta^E(\vec{k} \simeq 0, \eta_0, \mu, \hat{p}) = \theta_p (1 - \cos^2 \theta_{\vec{p}\vec{n}}) = \frac{2}{3} \theta_p - \frac{2}{3} \theta_p P_2(\cos \theta_{\vec{p}\vec{n}}) . \quad (3.34)$$

It is evident from Eq. (3.34) that the non-zero multipole coefficients $a_{\ell m}^E$ are for the monopole $\ell = 0$ and the quadrupole $\ell = 2$. The monopole term indicates a non-zero average large scale polarisation of the cosmic microwave background that can be evaluated as:

$$\left(\frac{\Delta T_0^{EE}}{T_0} \right)^2 \equiv \left(\frac{1}{4\pi} \int d\Omega \frac{\Delta T^E(\theta, \phi)}{T_0} \right)^2 \simeq \frac{4}{9} \theta_p^2 . \quad (3.35)$$

On the other hand, from Eq. (3.34) we easily obtain:

$$a_{2m}^E \simeq -\frac{8\pi}{15} \theta_p Y_{2m}^*(\theta_n, \phi_n) , \quad (3.36)$$

that implies:

$$\begin{aligned}
a_{20}^E &\simeq +\frac{1}{3}\theta_p\sqrt{\frac{\pi}{5}}[1+3\cos^2(2\theta_n)]\,, \\
a_{21}^E &= (a_{2,-1}^A)^* \simeq +2i\sqrt{\frac{\pi}{30}}\theta_p e^{-i\phi_n}\sin(2\theta_n)\,, \\
a_{22}^E &= (a_{2,-2}^A)^* \simeq +2\sqrt{\frac{\pi}{30}}\theta_p e^{-2i\phi_n}\sin^2\theta_n\,.
\end{aligned} \tag{3.37}$$

Using Eq. (3.37) we may easily estimate the quadrupole TE and EE correlations. For the quadrupole TE correlation we get:

$$\left(\frac{\Delta T_2^{TE}}{T_0}\right)^2 = \frac{3}{5\pi} \sum_{m=-2}^{m=+2} a_{2m}^A (a_{2m}^E)^* = \frac{3}{5\pi} \{a_{20}^A a_{20}^E + 2\mathcal{R}e[a_{21}^A (a_{21}^E)^*] + 2\mathcal{R}e[a_{22}^A (a_{22}^E)^*]\}\,, \tag{3.38}$$

where the a_{2m}^A 's are given by Eq. (3.13). Proceeding as in Ref. [20] one reaches the estimate:

$$\left(\frac{\Delta T_2^{TE}}{T_0}\right)^2 \simeq \frac{4}{5\sqrt{10}}\theta_p \mathcal{Q}_I \sin^2\theta_n \left[\cos(\phi_2 + 2\phi_n) + \frac{\sin^2\theta_n}{|\sin(2\theta_n)|}\right]. \tag{3.39}$$

For the quadrupole EE correlation we get:

$$\left(\frac{\Delta T_2^{EE}}{T_0}\right)^2 = \frac{3}{5\pi} \sum_{m=-2}^{m=+2} |a_{2m}^E|^2 \simeq \frac{16}{75}\theta_p^2. \tag{3.40}$$

From Eqs. (3.35), (3.39) and (3.40) it is straightforward to obtain:

$$(\Delta T_2^{TE})^2 \simeq 8.28 \pm 3.70 \mu K^2, \tag{3.41}$$

$$(\Delta T_0^{EE})^2 \simeq 1.26 \pm 0.80 \mu K^2, \tag{3.42}$$

$$(\Delta T_2^{EE})^2 \simeq 0.60 \pm 0.38 \mu K^2. \tag{3.43}$$

3.1 Comparison with the Planck 2018 data

Figure 1 summarises what we have achieved in this work. Indeed, in Fig. 1 we report TE (left panel) and EE (right panel) temperature correlations at large scales $\ell \leq 12$. It is worthwhile to observe that measuring the CMB polarisation signals at large angular scales is challenging due to the contamination from foreground sources. In general the main sources of foreground polarisation signals are synchrotron radiation, dust emission and thermal bremsstrahlung. To extract the underlying CMB signal, the foreground signal must be removed. The removal processes form a significant part of the CMB data analysis becoming increasingly important for the large-scale polarisation signals. The Planck team used component separation techniques to produce various maps of foregrounds. Foreground removal techniques make specific assumptions about the properties of foregrounds in temperature and in polarisation. To obtain a characterisation of the foregrounds that is independent of the component-separation methods, the Planck Collaboration, after subtracting from the observed power spectra the CMB contribution

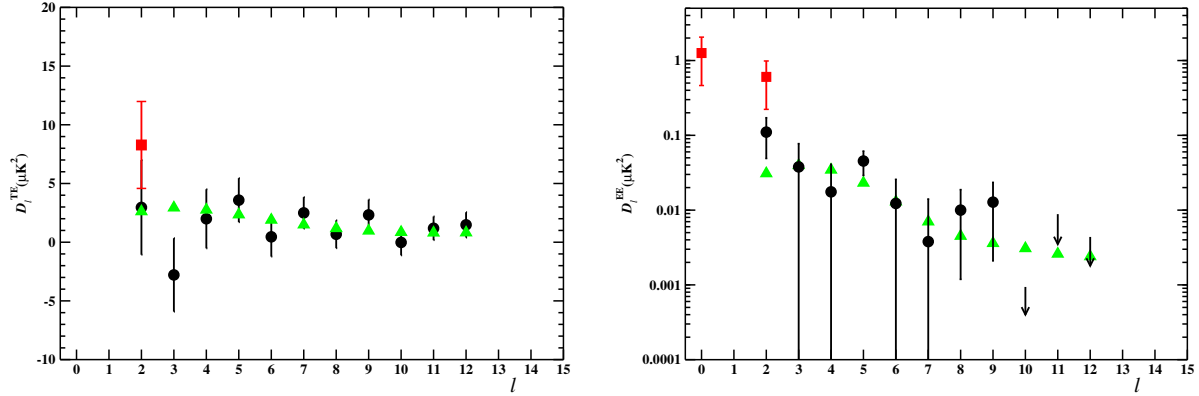


Figure 1: (color online) The TE (left panel) and EE (right panel) temperature correlations at large scales $\ell \leq 12$. Full (black) points are the latest Planck data. The arrows indicate the upper limits at 68 % confidence level. The full (green) triangles are the TE and TT temperature correlations of the Λ CDM best fit. The full (red) squares are our results Eqs. (3.41), (3.42) and (3.43).

determined by using the Planck 2015 Λ CDM model [29], performed a power-law fits to the power spectra over the multipole range $40 \leq \ell \leq 600$. After that, the extrapolation of the fitted power laws to the low multipoles was compared to the data points at $\ell < 40$ not used in the fit. It turned out that the extrapolation of the power laws to low multipoles was not always close to the data points [9]. This quantifies the challenge of the component-separation procedure that is required for measuring the low- ℓ primordial CMB E-modes. We see, then, that on the largest angular scales the Planck's results for the primordial CMB polarisation remain contaminated by astrophysical foreground and unknown systematic errors. The latest Planck data for the large-scale TE and EE power spectra are displayed in Fig. 1 as full points [26]. The data are affected by a rather large statistical uncertainties mainly due to the problematic component-separation procedures. Nevertheless, one can safely affirm that there is an evidence of primordial CMB polarisation signal at large scales. It is widely believed that the primordial CMB polarisation signal at large scales is due to the reionization processes. Even though the process by which the universe become fully reionized is still not well characterised, the reionization process is estimated to be complete at the redshift of reionization z_{re} . The best fit Λ CDM model gave $z_{re} = 7.67 \pm 0.67$ and Thomson optical depth $\tau = 0.0544 \pm 0.0073$ (see Table 2 in [2]). The resulting TE and EE multipole correlations are reported in Fig. 1 (full triangles). Looking at Fig. 1 it seems that the best fit model is in reasonable agreement with the Planck data within the rather large statistical errors. However, due to the measurement uncertainties there is no a clear evidence of the E-mode reionization bumps that should be around $\ell \simeq 3 - 4$ for a Thompson scattering optical depth $\tau \simeq 0.055$. On the other hand, we said that the ellipsoidal geometry of the universe induces sizeable polarisation signal at large scales even without invoking the reionization scenario. Our main results, given by Eqs. (3.41), (3.42) and (3.43), are compared to the Planck data in Fig. 1 (full squares). We see that our estimate of the quadrupole TE correlation is consistent with observations within the statistical errors. As concern the quadrupole EE correlation, our result Eq. (3.43) agrees with the data point at the same confidence level

as the best fit model. Moreover, in Ref. [20] we already argued that in our cosmological model the polarisation of the cosmic microwave background (without reionization) at the present time is essentially that produced around the time of recombination and, due to the finite thickness of the last scattering surface, it should be confined up to multipoles $\ell \lesssim 10$. In fact, this is confirmed in Ref. [17] where the authors have derived the radiative transfer equation in homogeneous anisotropic universes in the Bianchi VII_h case arguing that qualitatively the level of polarisation induced by the spatial anisotropy of the metric should hold also for Bianchi I anisotropic universes. Therefore, in our cosmological anisotropic model the polarisation signal should smoothly extend up multipoles $\ell \simeq 10$ and after that fall off very rapidly, in qualitative agreement with the Planck data. From the TE and EE power spectrum at large angular scales we see that the Bianchi-induced polarisation can mimic the effects of the early reionization of the standard cosmological model. Unfortunately, the Planck 2018 data on the large-scale polarisation are not yet able to distinguish between these two model. Nevertheless, a clear signature of the ellipsoidal universe model resides on the fact that, at variance of the standard reionization scenario, there is a non-zero average temperature polarisation. Our estimate of the average polarisation (monopole EE correlation) given by Eq. (3.42) is displayed in Fig. 1, right panel. In principle, the monopole EE correlation can be easily measured by averaging the polarisation signal over all directions. However, the lack of adequate theoretical models able to explain the foreground polarisation at large scales prevents, at moment, a reliable estimate of the average polarisation. In fact, the eventual presence of an average temperature polarisation could be misinterpreted as foreground emission leading to an underestimate of the cosmic microwave background polarisation signal.

4 Conclusions

The final results on the CMB anisotropies by the Planck Collaboration are confirming the cosmological Lambda Cold Dark Matter model to the highest level of accuracy. Nevertheless, at large angular scales there are still anomalous features in CMB anisotropies. Actually, the most evident discrepancy resides in the quadrupole TT correlation. The latest observed quadrupole TT correlation is:

$$(\Delta T_2^{TT})^2 = 225.90^{+533.06}_{-132.37} \mu K^2, \quad (4.1)$$

where the estimated errors take care of the cosmic variance. On the other hand, the 'TT,TE, EE + low E + lensing' best fit Λ CDM model to the Planck 2018 data gave:

$$(\Delta T_2^{TT})_{\Lambda CDM}^2 = 1016.73 \mu K^2, \quad (4.2)$$

that differs from the observed value by about two standard deviations. It has been suggested [10, 11] that, if one assumes that the large-scale spatial geometry of our universe is slightly anisotropic, then the quadrupole amplitude can be drastically reduced without affecting higher multipoles of the angular power spectrum of the temperature anisotropies [19, 20]. In the present paper, that relies heavily on our previous work, we performed a stringent comparison with the latest CMB data from the Planck Collaboration. As in previous papers we established that the low quadrupole temperature correlation, detected by WMAP and confirmed by the Planck satellite, could be accounted for if

the geometry of the universe is plane-symmetric with eccentricity at decoupling of order 10^{-2} . In fact, we fixed the eccentricity at decoupling, Eq. (3.29), and the polar angles of the direction of the axis of symmetry, Eq. (3.32), such that the quadrupole TT correlation matches exactly the observed value Eq. (4.1). As a consequence the ellipsoidal universe model seems to compare a little bit better than the standard cosmological Lambda Cold Dark Matter model. On the other hand, it is known since long time that anisotropic cosmological model could induce sizeable large-scale CMB polarisation. Indeed, we already argued that in the ellipsoidal universe model there is a sizeable polarisation signal at scales $\ell \lesssim 10$. Moreover, we showed that the quadrupole TE and EE correlations in the ellipsoidal universe are in reasonably agreement with the Planck 2018 data. Therefore, we are led to conclude that the proposal of the ellipsoidal universe cosmological model is still a viable alternative to the standard cosmological model. Finally, we suggested that a reliable estimate of the average large-scale polarisation by the Planck Collaboration could confirm or reject the ellipsoidal universe proposal.

References

- [1] N. Aghanim et al., Planck Collaboration, Planck 2018 results. III. High Frequency Instrument data processing and frequency maps, arXiv:1807.06207 [astro-ph.CO] (2018)
- [2] N. Aghanim et al., Planck Collaboration, Planck 2018 results. VI. Cosmological parameters, arXiv:1807.06209 [astro-ph.CO] (2018)
- [3] N. Aghanim et al., Planck Collaboration, Planck 2018 results. VIII. Gravitational lensing, arXiv:1807.06210 [astro-ph.CO] (2018)
- [4] N. Aghanim et al., Planck Collaboration, Planck 2018 results. XII. Galactic astrophysics using polarized dust emission, arXiv:1807.06212 [astro-ph.GA] (2018)
- [5] Y. Akrami et al., Planck Collaboration, Planck 2018 results. I. Overview and the cosmological legacy of Planck, arXiv:1807.06205 [astro-ph.CO] (2018)
- [6] Y. Akrami et al., Planck Collaboration, Planck 2018 results. II. Low Frequency Instrument data processing, arXiv:1807.06206 [astro-ph.CO] (2018)
- [7] Y. Akrami et al., Planck Collaboration, Planck 2018 results. IV. Diffuse component separation, arXiv:1807.06208 [astro-ph.CO] (2018)
- [8] Y. Akrami et al., Planck Collaboration, Planck 2018 results. X. Constraints on inflation, arXiv:1807.06211 [astro-ph.CO] (2018)
- [9] Y. Akrami et al., Planck Collaboration, Planck 2018 results. XI. Polarized dust foregrounds, arXiv:1801.04945 [astro-ph.GA] (2018)
- [10] L. Campanelli, P. Cea and L. Tedesco, Ellipsoidal Universe Can Solve the Cosmic Microwave Background Quadrupole Problem, Phys. Rev. Lett. **97**, 131302 (2006)
- [11] L. Campanelli, P. Cea and L. Tedesco, Cosmic microwave background quadrupole and ellipsoidal universe, Phys. Rev. D **76**, 063007 (2007)

- [12] P. J. E. Peebles, Principles of Physical Cosmology, Princeton University Press, Princeton (1993)
- [13] L. Bianchi, Sugli spazi a tre dimensioni che ammettono un gruppo continuo di movimenti, Mem. Mat. Fis. Soc. It. Sci., serie **III**, **Tomo XI**, 267 (1898); English translation: On three dimensional spaces which admit a group of motions, Gen. Rel. Grav. **33**, 2157 (2001)
- [14] M. J. Rees, Polarization and Spectrum of the Primeval Radiation in an Anisotropic Universe, Astrophys. J. **153**, L1 (1968)
- [15] J. Negroponte and J. Silk, Polarization of the Primeval Radiation in an Anisotropic Universe, Phys. Rev. Lett. **44**, 1433 (1980)
- [16] M. M. Basko and A. G. Polnarev, Polarization and anisotropy of the relic radiation in an anisotropic universe, Monthly Not. R. Astron. Soc. **191**, 207 (1980)
- [17] A. Pontzen and A. Challinor, Bianchi model CMB polarization and its implications for CMB anomalies, Monthly Not. R. Astron. Soc. **380**, 1387 (2007)
- [18] P.A.R. Ade et al., BICEP2/Keck and Planck Collaborations, Joint Analysis of BICEP2/Keck Array and Planck Data, Phys. Rev. Lett. **114**, 101301 (2015)
- [19] P. Cea, On the large-scale cosmic microwave background polarization, Monthly Not. R. Astron. Soc. **406**, 586 (2010)
- [20] P. Cea, The ellipsoidal universe in the Planck satellite era, Monthly Not. R. Astron. Soc. **441**, 1646 (2014)
- [21] C.L. Bennett et al., Nine-year Wilkinson Microwave Anisotropy Probe (WMAP) Observations: Final Maps and Results, Astrophys. J. Suppl. **208**, 20 (2013)
- [22] G.F. Hinshaw et al., Nine-year Wilkinson Microwave Anisotropy Probe (WMAP) Observations: Cosmological Parameter Results, Astrophys. J. Suppl. **208**, 19 (2013)
- [23] S. Dodelson, *Modern Cosmology*, Academic Press, San Diego, California (2003)
- [24] V. Mukhanov, *Physical Foundation of Cosmology*, Cambridge University Press, New York (2005)
- [25] S. Chandrasekhar, *Radiative Transfer*, Dover Publications, New York (1960)
- [26] Planck 2018: <https://www.cosmos.esa.int/web/planck>
- [27] D. J. Fixsen, The Temperature of the Cosmic Microwave Background, Astrophys. J. **707**, 916 (2009)
- [28] P. A. R. Ade et al., Planck Collaboration, Planck 2015 results. XVI. Isotropy and statistics of the CMB, Astron. Astrophys. **594**, A16 (2016)
- [29] P. A. R. Ade. et al., Planck Collaboration, Planck 2015 results. XIII. Cosmological parameters, Astron. Astrophys. **594**, A13 (2016)